

Scheme 1. Suggested mechanism for the $M[N(SiMe_3)_2]_3$ -catalyzed Tishchenko reaction.

that $1/[reactant]$ is related linearly to the reaction time; that is, a second-order reaction with respect to the reactant occurs. Such reaction kinetics have already been established for the aluminum-catalyzed reaction for the dimerization of benzaldehyde.^[9] Presumably, a molecule of the reactant coordinates to **A** (\rightarrow **B**), which in turn undergoes an alkoxide transfer (\rightarrow **C**; Scheme 1). A second molecule of the reactant attaches itself to **C** followed by a hydride transfer that is probably the rate-determining step (\rightarrow **D**).^[9]

In summary it should be emphasized that the bis(trimethylsilyl)amide compounds of the lanthanides represent a new class of Tishchenko catalysts as a result of the high Lewis acidity and the easy interchangeability of the ligand sphere. These compounds are distinguished by a number of practical advantages such as the ease of accessibility (one compound can be bought), inexpensive metals, extremely high activities (to our knowledge there are no catalysts that are more active), and a high durability of the catalysts. These advantages lead us to hope that **1**, which is already today a standard reagent in organolanthanide chemistry, will find further application as a Tishchenko catalyst.

Experimental Section

NMR-scale reaction: Compound **1** (0.015 mmol) was weighed under protective gas into an NMR tube. C_6D_6 (≈ 0.7 mL) was condensed into the NMR tube, and the mixture was frozen at $-196^\circ C$. The reactant (1.5 mmol) was injected onto the solid mixture, and the whole sample was frozen at $-196^\circ C$. To determine the reaction kinetics the sample was melted and mixed just before the insertion into the core of the NMR machine (t_0). The ratio between the reactant (product) and the catalyst was exactly calculated by comparison of the integration of all CHO (CH_2O) signals with the $N(SiMe_3)_2$ signals. The latter were used as an internal standard for the kinetic measurements.

Preparative-scale reaction: a) without solvent: Under protective gas the catalyst (1 mol %) was stirred in a tempered reaction flask. The reactant (5 g) was added directly to the catalyst. Usually an exothermic reaction was observed. After one day the product was isolated by distillation. b) In solution: The catalyst (1 mol %) and the reactant (5 g) were each dissolved in pentane/hexane (1/1, 25 mL). The reactant solution was added together

with the catalyst solution in a tempered flask. After one day the product was isolated by distillation.

Received: January 26, 1998 [Z11402IE]
German version: *Angew. Chem.* **1998**, *110*, 1618–1620

Keywords: aldehydes • homogeneous catalysis • lanthanides

- [1] a) L. Claisen, *Ber. Dtsch. Chem. Ges.* **1887**, *20*, 646–650; b) W. Tishchenko, *Chem. Zentralbl.* **1906**, *77*, I, 1309.
- [2] a) E. G. E. Hawkins, D. J. G. Long, F. W. Major, *J. Chem. Soc.* **1955**, 1462–1468, quote patent; b) F. R. Frostick, B. Phillips (Union Carbide & Carbon Corp.), US-A 2716123, **1953** [*Chem. Abstr.* **1953**, *50*, 7852f].
- [3] a) W. C. Child, H. Adkins, *J. Am. Chem. Soc.* **1923**, *47*, 789–807; b) F. J. Villani, F. F. Nord, *ibid.* **1947**, *69*, 2605–2607; c) L. Lin, A. R. Day, *ibid.* **1952**, *74*, 5133–5135.
- [4] P. R. Stapp, *J. Org. Chem.* **1973**, *38*, 1433–1434.
- [5] a) S. Onozawa, T. Sakakura, M. Tanaka, M. Shiro, *Tetrahedron* **1996**, *52*, 4291–4302; b) K.-I. Morita, Y. Nishiyama, Y. Ishii, *Organometallics* **1993**, *12*, 3748–3752; c) T. Ito, H. Horino, Y. Koshiro, A. Yamamoto, *Bull. Chem. Soc. Jpn.* **1982**, *55*, 504–512; d) M. Yamashita, T. Ohishi, *Appl. Organomet. Chem.* **1993**, *7*, 357–361.
- [6] D. C. Bradley, J. S. Ghorta, F. A. Hart, *J. Chem. Soc. Dalton Trans.* **1973**, 1021–1023.
- [7] Review: R. Anwander, *Top. Curr. Chem.* **1996**, *179*, 33–112.
- [8] D. A. Evans, A. H. Hoveyda, *J. Am. Chem. Soc.* **1990**, *112*, 6447–6449.
- [9] Y. Ogata, A. Kawasaki, *Tetrahedron* **1969**, *25*, 929–935.
- [10] As a catalyst for the dimerization of benzaldehyde, $Al(OCH_2Ph)_3$ is ten times faster than $Al(OiPr)_3$, because here the metal has already exchanged all $OiPr$ for OCH_2Ph groups.^[9] Although $Al(OCH_2Ph)_3$ is faster than $Al(OiPr)_3$ for this reaction, one cannot assume that this is always the case. For our comparative studies we were not interested in a special reaction, but rather in a wider application. Thus the literature quoted is almost exclusively with $Al(OiPr)_3$ as the catalyst.^[3, 11a]
- [11] a) G. Fouquet, F. Merger, R. Platz, *Liebigs Ann. Chem.* **1979**, 1591–1601; b) G. M. Villacorta, J. San Filippo, Jr., *J. Org. Chem.* **1983**, *48*, 1151–1154.

NaSn₅: An Intermetallic Compound with Covalent α -Tin and Metallic β -Tin Structure Motifs

Thomas F. Fässler* and Christian Kronseder

Under standard conditions tin exists in the β modification, in which each tin atom is surrounded by six other Sn atoms in a distorted octahedral arrangement (Figure 1a, Scheme 1, Table 1). Below $13.2^\circ C$ transformation of β -tin into cubic α -tin (diamond structure), which is thermodynamically more stable by 2.09 kJ mol⁻¹, occurs.^[1] In this modification, which has a lower density, all tin atoms are four-coordinate, and the structure can be described by invoking localized two-center, two-electron ($2c-2e$) bonds (Scheme 1). All structurally

[*] Dr. T. F. Fässler, C. Kronseder
Laboratorium für Anorganische Chemie der
Eidgenössischen Technischen Hochschule Zürich
Universitätsstrasse 6, CH-8092 Zürich (Switzerland)
Fax: (+41)1-632-1149
E-mail: faessler@inorg.chem.ethz.ch

[**] This work was supported by the Eidgenössische Technische Hochschule Zürich.

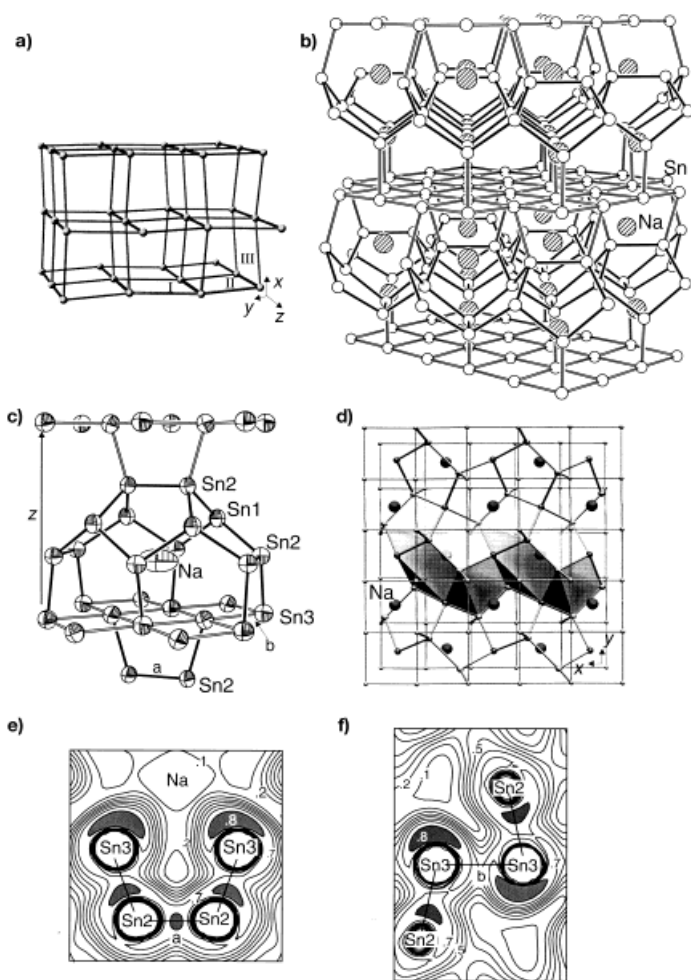
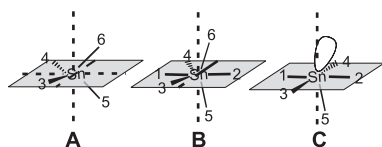


Figure 1. a) Section of the β -Sn structure. The atoms lie in layers parallel to the xz and xy planes. The shaded parallelograms are coplanar (I and II) or orthogonal (II and III; see **B** in Scheme 1). b)–d) Sections of the structure of NaSn_5 . b) A larger section showing the stacking of the five-membered ring units. c) The twelve Sn atoms of this section (Sn1 and Sn2 atoms) are not part of the quadratic network and form a polyquinane-like structural unit. When the eight bridging atoms of the quadratic network below are included, this unit is topologically equivalent to a pentagonal dodecahedron (see Scheme 2). The anisotropic displacement parameters are drawn at the 90 % probability level. d) Both shaded tub units are shown with their openings facing downwards. The convex indentations in a translationally symmetric arrangement of concave tub units are themselves tub units. Their openings face upwards and, along with the former units, completely fill the space between the quadratic networks. Distances and angles are given in Scheme 1 and the text. e) and f) The electron localization function (ELF) of cross-sections in the NaSn_5 structure parallel to the z direction and through the bonds labeled a and b in c). The ELF is normalized to values between 0 and 1. The contour lines are in steps of $\text{ELF} = 0.1$. In e) one can clearly recognize a preferential orientation of the electron lone pairs of the Sn3 atoms (see text for details).



Scheme 1. Distances and angles in α -Sn (**A**), β -Sn (**B**), and in the coordination sphere of Sn3 in NaSn_5 (**C**). **A**: 2.810 \AA ($4 \times$); 109.5° ($6 \times$); **B**: Sn–Sn(3) to Sn–Sn(6) 3.016 , Sn–Sn(1) and Sn–Sn(2) 3.175 \AA ; **C**: Sn3–Sn(1) to Sn3–Sn(4) 3.143 , Sn3–Sn(5) 2.886 \AA ; the angles between the Sn atoms in **B** and **C** are listed in Table 1.

characterized tin-rich binary alkali metal stannides are, like α -tin, covalent compounds. According to the Zintl–Klemm–Busmann (ZKB) concept, the valence electrons of the electropositive alkali metal atoms are assigned to the tin atoms, and the number of three- and four-coordinate tin atoms and homoatomic bonds is determined by the $8 - N$ rule. The three-coordinate atoms carry a negative charge or a lone pair. The anionic substructures in ASn (i.e., A_4Sn_4 , $\text{A} = \text{Na} - \text{Rb}$; NaPb type),^[2] $\text{A}_8\text{Sn}_{44}\square_2$ ($\text{A} = \text{K}, \text{Cs}$, clathrate I structure type with two vacancies),^[3] and the recently reported

Table 1. Sn–Sn–Sn bond angles [$^\circ$] in structures **B** and **C**.

	3–4	5–6	1–3	1–4	2–3	2–4	1–5(6)	2–5(6)	3–5(6)	4–5(6)
B	149.5	149.5	74.8	74.8	105.2	105.2	105.2	74.8	94.0	94.0
C	178.0	–	89.0	90.0	90.0	91.0	102.2	79.5	102.2	79.5

$\text{Na}_5\text{Sn}_{13}$ ^[4] can be described by formulating localized $2c-2e$ bonds and electron lone pairs. In addition to the three-membered tin rings of the tetrahedral cluster in ASn ,^[5] five-membered tin rings are the predominant structural motif. In $\text{Na}_5\text{Sn}_{13}$ these are assembled by edge sharing and external bonds to form a complex three-dimensional network; in the clathrate I structure type they appear as building blocks of pentagonal dodecahedra. The four-coordinate atoms in these structures have a distorted tetrahedral environment. The bonding motifs of the metallic tin modification are not reflected in any of the known intermetallic tin compounds.^[7]

Here we report on NaSn_5 , the most tin-rich phase of the Na–Sn system. This is the first example of a tin network in which fragments of pentagonal dodecahedra with tetravalent atoms are bound between planar networks of tin atoms. The tin atoms of the planar network have a distorted square-pyramidal coordination to five other tin atoms. These build, together with a free electron pair localized on the central tin atom, a distorted ψ -octahedral coordination polyhedron. A similar polyhedron occurs in the β -tin structure.

Single crystals^[8] of NaSn_5 were obtained by combination of the elements.^[9] The compound crystallizes in a new structure type with three independent Sn positions and one Na position (Pearson symbol tP12, Figure 1 b–d). The Sn3 atoms build a planar, mildly distorted quadratic network (Sn3–Sn3 $3.1429(5) \text{ \AA}$), and the Sn1 and Sn2 atoms form a fragment of a pentagonal dodecahedron (Figure 1 c). The twelve atoms of the latter unit are constructed from four five-membered rings with five shared edges. The result is a tublike half-shell with C_{2v} point symmetry that can be derived from the analogous polyquinane hydrocarbon.^[10] The tub can also be described as a ten-membered chain bridged by a handle. The bridging handle of Sn2 atoms and the six symmetry-equivalent atoms of the ten-membered chain (Sn2) are bound to the atoms of the quadratic network (Sn2–Sn3 $2.886(1) \text{ \AA}$). The polyhedral fragment spans eight Sn3 atoms (Figure 1 c). The relative arrangement of a fragment between two planar networks is detailed in Figure 1 d. The two-dimensional connectivity of the fragments leads to a layer of four-coordinate atoms that alternate along the z direction with the quadratic network (Figure 1 b). A layered arrangement of

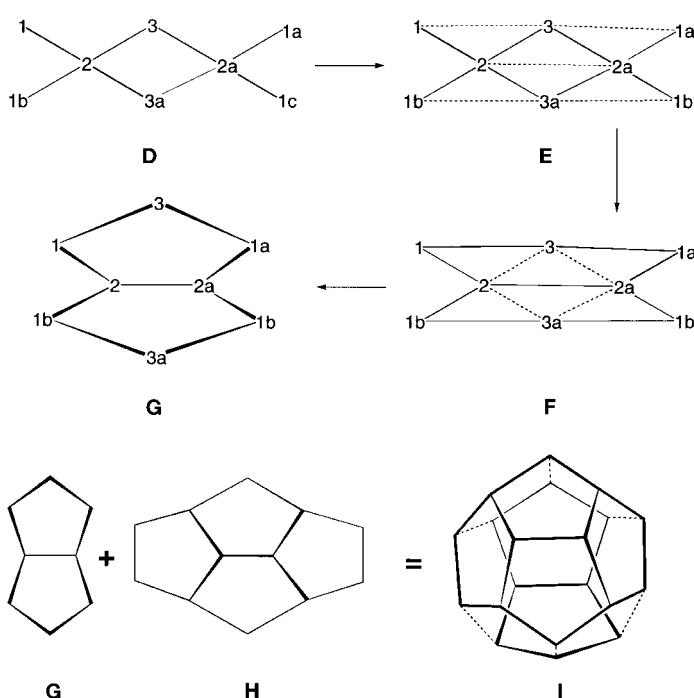
linked five-membered ring units is also present in the Zintl phases $\text{Li}_7\text{Ge}_{12}$ and Li_3NaSi_6 .^[11]

The Sn1 and Sn2 atoms are four-coordinate. The environment of Sn1 deviates only slightly from a tetrahedral arrangement: Sn1–Sn2 2.8626(6) Å; bond angles at Sn1 range from 108.32(1) to 111.80(3)°; Sn2–Sn3 2.886(1) Å; bond angles at Sn2 range from 101.94(2) to 117.25(2)°. The center of each tub is occupied by a Na atom, which exhibits short interatomic distances to two Sn2 atoms (3.054(1) Å);^[12] the next-nearest neighbors are Sn2 atoms at distances of 3.409(6) and 3.415(6) Å ($2\times$), Sn1 atoms at a distance of 3.625(4) Å ($4\times$), and two further Sn2 atoms (the Sn2 atoms of the bridging handle, Figure 1c) at a distance of 3.687(8) Å ($2\times$). Four other Sn2 atoms exhibit even longer distances of 4.663 Å.

The Sn3 atoms have a coordination environment similar to that in metallic tin. In β -Sn the atoms lie in sheets parallel to the xz and xy planes, composed of parallelograms with angles of 74.8 and 105.2° (Figure 1a). The Sn–Sn bond lengths are 7 and 13 % longer than those of α -tin. Bond lengths and angles are given in Scheme 1 and Table 1. The planar networks in NaSn_5 are constructed from quadratic units. The distances between the network atoms are 12 % greater than the corresponding distances in α -tin. If Sn3 is described with an electron lone pair that is regarded as a pseudoligand according to the VSEPR rules, the resulting environment about the Sn3 atom is analogous to that in β -tin. The axial positions (see Scheme 1) 5 and 6 in **B**, and 5 and an electron lone pair in **C**, are distorted from an ideal octahedral arrangement in the direction of position 2 and the bisector of the angle Sn(2)–Sn–Sn(4), respectively.

The chemical bonding in NaSn_5 is interesting in two distinct ways. First, the title compound exhibits a topological transition from the coordination in β -tin to pentagonal-dodecahedral units; such units are present in the clathrate I structure, K_6Sn_{25} , and $\text{K}_6\text{Sn}_{23}\text{Bi}_2$. The latter two phases crystallize in the $\text{Ba}_6\text{In}_4\text{Ge}_{21}$ ^[6a, 14] structural type and contain distorted pentagonal dodecahedra of the elements Sn^[3b, 15] and Sn/Bi^[15] in place of In/Ge. These pentagonal dodecahedra form three-dimensional zeolite-like networks in which each shares three faces and has one exo bond.^[14, 16] The development of such polyhedra from the β -Sn structure is especially striking in the NaSn_5 structure. In Scheme 2 the transformation of the C_{2v} -symmetric hemisphere (comprising $12 + 8 = 20$ Sn atoms) to a pentagonal dodecahedron is shown. The distortion of the quadratic network of eight Sn atoms (**D**), which borders the fragment **H**, passes through the intermediates **E** and **F** to form two edge-sharing five-membered rings (**G**, pentalene analogue). One of these supplements the fragment **H** to create a pentagonal dodecahedron (**I**). Furthermore, NaSn_5 contains both localized bonds between tetravalent atoms, as in α -tin and the Zintl phases, and delocalized bonds like those of β -tin. The structural findings discussed above were verified with band structure calculations.

LMTO-ASA calculations^[18] predicted NaSn_5 to be an anisotropic conductor. The density of states at the Fermi level E_F can be attributed predominantly to contributions from the Sn3 atoms (Figure 2, right). The fat-band analysis, in which the atomic orbital character is represented as a function



Scheme 2. The topological transformation from eight atoms of a quadratic network and a unit of four five-membered rings to a pentagonal dodecahedron. In **D**, a section from a quadratic network, a connection along the diagonal, as shown in **E**, is effected. Opening of the dashed lines in **F** with a concomitant distancing of the centers 3 and 3a leads to two edge-sharing five-membered rings (**G**). The fragments **G** and **H** combine to form a pentagonal dodecahedron **I**.

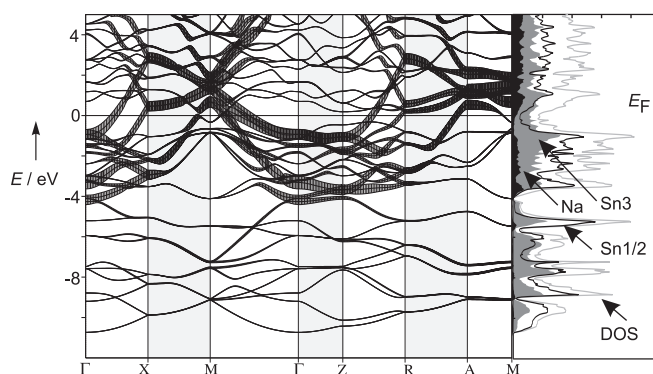


Figure 2. Band structure showing p_x and p_y orbital character (fat-band analysis),^[18] density of states (DOS), and the atomic contributions to the DOS.

of the band width, shows that the bands crossing the Fermi level are characterized almost completely by contributions from the p_x and p_y orbitals of Sn3; that is, metallic conductivity propagates predominantly over states with Sn3 orbital contributions. The presence of structural regions with delocalized bonds, the localized bonds of the tetravalent Sn1 and Sn2 atoms, and the electron lone pairs on the Sn3 atoms (see Scheme 1) is further supported by analysis of the quantum-mechanical results with the help of the electron localization function (ELF).^[19]

Cross-sectional plots of the ELF in two planes parallel to the z direction and through the Sn2–Sn2 bond a (along [110])

and the Sn3–Sn3 bond b ([100]) are shown as contour diagrams in Figures 1e and 1f. Regions with ELF greater than 0.8 characteristic of 2c–2e bonds can be clearly recognized between the atom pairs Sn2–Sn2 and Sn2–Sn3. The ELF region along the Sn2–Sn3 bond is typical of a polar bond.^[19c] Not depicted are the regions of higher ELF values, which show another 2c–2e bond along the Sn1–Sn2 interaction vector. The localization is clearly poorer (ELF < 0.6) between the Sn3 atoms, and the ELF shows no local maximum (attractor^[19d]) on the nucleus–nucleus connecting line (Figure 1f). A electron lone pair on the Sn3 atom is clearly apparent (Figure 1e); it is directed toward the electropositive Na atoms and together with the five other bound Sn atoms builds a distorted octahedral coordination polyhedron about Sn3. The comparison with the coordination of the Sn atoms in metallic tin is highlighted in Scheme 1. When the electrons in NaSn₅ are distributed according to the ZKB concept, the formula Na₂(Sn1)₂(Sn2)₄(Sn3)₄ results with a partial charge of –0.5 on Sn3.^[20] Since two electrons are considered to form the lone pair, 0.75 electrons per shortest Sn3–Sn3 distance remain for the bonds of the quadratic network. This is consistent with 4c–3e bonds between the atoms of the planar network. BaAl₄, in which Al atoms cap quadratic nets of Al atoms, has 6e–5c bonds between the network and apical atoms, and the ELF values between the atoms of the Al networks are also small (ELF < 0.6).^[21]

NaSn₅ represents a new, unusual three-dimensional network in which metallic layers analogous to those in β-tin alternate with tetravalent tin atoms. The compound shows the beginning of the formation of pentagonal-dodecahedral units (which frequently occur in Zintl phases) from the β-Sn modification. Like the recently reported stannide BaSn₃, the title compound lies on the border between Zintl phases and intermetallic compounds. Interesting physical properties are predicted on the basis of theoretical calculations.^[6b] The determination of the electronic properties and a more thorough quantitative analysis of the chemical bonding with the aid of the ELF (electronic domains)^[21b] are the subject of further investigations.

Received: December 2, 1997 [Z112251E]

German version: *Angew. Chem.* **1998**, *110*, 1641–1644

Keywords: bond theory • intermetallic phases • tin • Zintl phases

- [1] A. F. Hollemann, E. Wiberg, *Lehrbuch der anorganischen Chemie, Hollemann-Wiberg*, de Gruyter, Berlin **1995**.
- [2] R. E. Marsh, D. P. Shoemaker, *Acta Crystallogr.* **1953**, *6*, 197; I. F. Hewaidy, E. Busmann, W. Klemm, *Z. Anorg. Allg. Chem.* **1964**, *328*, 283.
- [3] a) J. Gallmeier, H. Schäfer, A. Weiss, *Z. Naturforsch. B* **1969**, *24*, 655; b) Y. N. Grin, L. Z. Melekhov, K. A. Chuntanov, S. P. Yatsenko, *Sov. Phys. Crystallogr.* **1987**, *32*, 290; c) J. Zhao, J. D. Corbett, *Inorg. Chem.* **1994**, *33*, 5721; d) Na₈Si₄₆ type: J. S. Kasper, P. Hagenmuller, M. Pousard, C. Cros, *Science*, **1965**, *150*, 1713; e) the clathrate I structure type was originally described with the composition A₈E₄₆ (E = Si–Sn). The correct composition, A₈E₄₄, results from two vacancies per formula unit and gives a partial tin structure with three- and four-coordinate atoms, which is consistent with the 8–N rule: H. G. von Schnering, *Nova Acta Leopoldina* **1985**, *59*, 168.
- [4] J. T. Vaughey, J. D. Corbett, *Inorg. Chem.* **1997**, *36*, 4316.
- [5] In BaSn₃,^[6a] three-membered rings of Sn atoms form the building block for chains of face-sharing octahedra. BaSn₃ is a superconductor and may be described as a Zintl phase with strongly interacting 2π aromatic Sn₃^{2–} anions (Sn–Sn 3.058 (2 ×), 3.266 Å (4 ×)).^[6b]
- [6] a) R. Kröner, Dissertation, Universität Stuttgart, **1989**; b) T. F. Fässler, C. Kronseder, *Angew. Chem.* **1997**, *109*, 2800; *Angew. Chem. Int. Ed. Engl.* **1997**, *36*, 2683.
- [7] Coordination numbers greater than four also occur in BaSn₃^[10] and in the discrete Sn_n^{2–} (n = 5, 6, 9) Zintl anions. For examples, see J. D. Corbett, *Struct. Bonding (Berlin)* **1997**, *87*, 157; B. Schiemenz, G. Huttner, *Angew. Chem.* **1993**, *105*, 295; *Angew. Chem. Int. Ed. Engl.* **1993**, *32*, 297; T. F. Fässler, M. Hunziker, *Z. Anorg. Allg. Chem.* **1996**, *622*, 837; H. G. von Schnering, M. Baitinger, U. Bolle, W. Carrillo-Cabrera, J. Curda, Y. Grin, F. Heinemann, J. Llanos, K. Peters, A. Schmeding, M. Somer, *ibid.* **1997**, *623*, 1037.
- [8] Crystal structure analysis of NaSn₅: A needle of dimensions 0.20 × 0.12 × 0.48 mm was mounted in a glass capillary. Cell constants at T = 293 K: a = b = 6.2992(1), c = 8.8172(2) Å; V = 349.9(1) Å³; space group P4₂m (no. 113), Z = 2. ρ_{calc} = 5.893 g cm^{–3}, μ = 17.66 mm^{–1}. Data collection: STOE IPDS, MoK_α radiation, 2θ_{max} = 56.38° (detector distance 60 mm), 3663 reflections, 479 independent reflections (R_{int} = 0.066). Absorption effects were taken into account by using the program ABCOR (STOE program suite). The structure was solved by direct methods (SHELXS-86). A full-matrix least-squares refinement on F² allowing for anisotropic motion of all atoms (SHELXL-96) converged to R₁ = 0.025 and wR = 0.059 for 20 parameters and 466 reflections with I > 2σ(I). Residual electron density: 1.115/–0.963 e Å^{–3}. The Na atom has a large displacement parameter relative to the Sn atoms (Figure 2c). The electron-density map does not indicate a split position. The possibility of an under-occupied Na site or presence of oxygen appears to be unlikely according to the appropriate refinements. Further details of the crystal structure investigations may be obtained from the Fachinformationszentrum Karlsruhe, D-76344 Eggenstein-Leopoldshafen, Germany (fax: (+49) 7247-808-666; e-mail: crysdata@fiz-karlsruhe.de), on quoting the depository number CSD-408045.
- [9] A single crystal was isolated from a reaction with Na:Sn = 1.2:5. The reaction was performed in a welded niobium ampoule placed in an evacuated quartz tube. The reaction mixture was heated at 150 °C h^{–1} to 620 °C, held at that temperature for 5 h, and subsequently cooled at 50 °C h^{–1} to room temperature. In addition to peaks matching the calculated powder diagram of NaSn₅, the powder diagram of the product of a stoichiometric reaction shows peaks of weaker intensity corresponding to elemental tin and lines of a hitherto unidentified phase. The silver-gray product has a laminar structure and is relatively easily exfoliated in one direction; it is very hard in the perpendicular direction.
- [10] M. Venkatachalam, M. N. Deshpande, M. Jadowski, G. Kubiak, S. Wehrli, J. M. Cook, U. Weiss, *Tetrahedron* **1986**, *42*, 1597. A. Nickon, E. F. Silversmith, *Organic Chemistry, The Name Game*, Pergamon Press 1987. L. A. Paquette, *Top. Curr. Chem.* **1984**, *119*, 1.
- [11] R. Nesper, *Prog. Solid St. Chem.* **1990**, *20*, 1.
- [12] On taking into account the anisotropic displacement parameters of the Na atom^[8] an Na–Sn2 interatomic distance of 3.13 Å results.^[13] Comparatively short Na–Sn interatomic distances (3.17 Å) are found in Na₅Sn₁₃^[4] and Na₉Sn₄: W. Müller, K. Volk, *Z. Naturforsch.* **1978**, *33b*, 275.
- [13] SHELXTL Version 5, Reference Manual, Siemens Analytical X-Ray Systems, Inc, **1996**.
- [14] R. Kröner, R. Nesper, H. G. von Schnering, *Z. Kristallogr.* **1988**, *182*, 164.
- [15] T. F. Fässler, C. Kronseder, *Z. Anorg. Allg. Chem.* **1998**, *624*, 561.
- [16] There are 17 four-coordinate and 8 three-coordinate framework atoms per formula unit; hence, the ternary compounds can be described as Zintl phases. The geometric arrangement of eight electron lone pairs requires raising the energy of a state (band) in the tin-rich phase. This band comprises orbital character from all eight free electron pairs. If, as is the case in K₆Sn₂₅, this band is not fully occupied, a corresponding under-occupation of all eight electron pairs follows. In this light, K₆Sn₂₅ may be considered an electron-poor Zintl

phase.^[17] A compound with the composition $K_{7.4}Sn_{25}$ has also been discussed.^[3c]

- [17] T. F. Fässler, *Z. Anorg. Allg. Chem.* **1998**, 624, 569.
 [18] LMTO-ASA (linear muffin-tin orbital in the atomic sphere approximation): M. van Schilfgarde, T. A. Paxton, O. Jepsen, O. K. Andersen, G. Krier, unpublished TB-LMTO program, Max-Planck-Institut für Festkörperforschung, Stuttgart **1994**; U. Barth, L. Hedin, *J. Phys. Chem.* **1972**, 5, 1629; O. Jepsen, O. K. Andersen, *Z. Phys. B* **1995**, 97, 35.
 [19] a) A. D. Becke, E. Edgecombe, *J. Chem. Phys.* **1990**, 92, 5397; A. Savin, A. D. Becke, J. Flad, R. Nesper, H. G. von Schnering, *Angew. Chem.* **1991**, 103, 421; *Angew. Chem. Int. Ed. Engl.* **1991**, 31, 185; b) A. Savin, R. Nesper, S. Wengert, T. F. Fässler, *ibid.* **1997**, 109, 1892 and **1997**, 36, 1808; c) T. F. Fässler, A. Savin, *Chem. unserer Zeit* **1997**, 31, 110; d) B. Silvi, A. Savin, *Nature* **1994**, 371, 683.
 [20] According to this charge distribution, one would expect the shortest distances to be found between the Na and Sn3 atoms. A shortening of the Na–Sn distances would result in lengthening of the Na–Sn1 distances;^[4] these are already relatively long (3.625 Å), even for four-coordinate tin atoms.
 [21] a) U. Häussermann, S. Wengert, P. Hofmann, A. Savin, O. Jepsen, R. Nesper, *Angew. Chem.* **1994**, 106, 2147; *Angew. Chem. Int. Ed. Engl.* **1994**, 33, 2069; b) U. Häussermann, S. Wengert, R. Nesper, *ibid.* **1994**, 106, 2150 and **1994**, 33, 2073.

Small Potassium Clusters**

Andreas Kornath*, Ralf Ludwig, and Anja Zoerner

The investigation of ligand-free atomic clusters presents an ideal opportunity for studying the transition from a single atom to a macroscopic particle. Moreover, the basic properties of small metallic clusters are believed to be an important link in the understanding of the fundamental mechanisms of catalysis and numerous chemical transformations.^[1] Despite considerable recent effort, the structures of small atomic metal clusters remain largely unknown.^[2, 3] This attests to the intrinsic difficulties associated with experimental work in this field. Even the generation and isolation of the smallest species requires an extensive experimental setup.^[4] On the other hand, the number of theoretical calculations and predictions has increased explosively during this decade due to the increasing computer capacity available. Alkali metal clusters are one of the main subjects for theoretical work, but even the diatomic species have yet to be isolated experimentally.

A simplified method for the generation of diatomic potassium molecules was developed during experiments for the simulation of stratospheric phenomena. The apparatus consists of a regular low-pressure plasma tube which is connected to a cryostat with a copper cold surface (15 K).^[5]

[*] Dr. A. Kornath, Dr. R. Ludwig, Dipl.-Chem. A. Zoerner
 Anorganische Chemie, Fachbereich Chemie der Universität
 Otto-Hahn-Strasse 6, D-44221 Dortmund (Germany)
 Fax: (+49) 231-755-3797
 E-mail: kornath@citrus.chemie.uni-dortmund.de

[**] Raman Matrix Isolation Spectroscopy, part 7. We would like to thank Prof. R. Minkwitz and the Deutsche Forschungsgemeinschaft for support of this work. Part 6: A. Kornath, *J. Mol. Spectrosc.* **1998**, 188, 63–67.

The metal sample is sputtered by a microwave-induced low-pressure krypton plasma, and the material stream is frozen immediately on the cold surface. After one hour of deposition time, a blue layer of solid krypton and potassium molecules was formed. Figure 1 shows the Raman spectrum of the

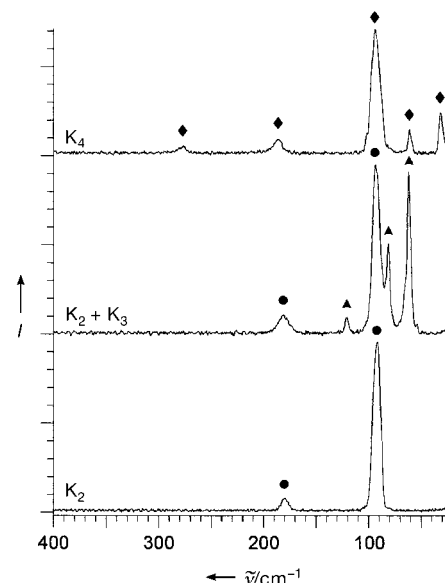


Figure 1. Raman matrix spectra of K_2 , K_4 , and a mixture of K_2 and K_3 in krypton at 15 K (experimental conditions: 100 μ m layer, laser wavelength 514.5 nm, laser power 125 mW, resolution 0.6 cm^{-1}). I = intensity. ●: lines from K_2 , ▲: from K_3 , ◆: from K_4 .

krypton matrix with diatomic potassium molecules. The fundamental frequency of 91.0 cm^{-1} is in excellent agreement with the value obtained from gas-phase experiments (92.0 cm^{-1}), and from density functional theory (DFT) calculations (see Table 1).^[6] The surprising result of the microwave sputtering experiment is the efficient formation of the diatomic species. Thermal evaporation under similar conditions (ca. 80 °C) would yield more than 99 % potassium atoms.^[7] This was verified by thermal evaporation experiments which yielded red matrices of potassium atoms without any detectable molecular species. These experiments also confirm that the blue color of the krypton matrix is due to the

Table 1. Experimental and calculated (DFT) Raman frequencies [cm^{-1}], and vibration modes for K_2 , K_3 , and K_4 .

K_n	DFT ^[a]	Exp.	Assignment
K_2	90.0	91.0	$\nu(K_2)$ Σ_g
		181.5	$2\nu(K_2)$ Σ_g
K_3	57.2	(61.0)	$\delta(K_3)$ A_1
	58.9	61.0	$\delta(K_3)$ B_2
	83.0	81.5	$\nu(K_3)$ A_1
		120.0	$2\delta(K_3)$ A_1
K_4	31.2	30.0	$\delta(K_4)$ A_g
	60.0	61.5	$\delta(K_4)$ B_{3g}
	92.4	93.0	$\nu(K_4)$ A_g
		185.0	$2\nu(K_4)$ A_g
		276.0	$3\nu(K_4)$ A_g

[a] DFT calculations with the Slater exchange function and the local spin density correlation function of Vosko, Wilk, and Nusair (SVWN5)^[10] and the basis set LANL2DZ^[11] performed with the Gaussian 94 package.^[16]